# Field-correlation effects on Raman-enhanced nondegenerate four-wave mixing

Zuhe Yu, Xin Mi, Qian Jiang, Xiaofeng Li, and Panming Fu*
*Laboratory of Optical Physics, Institute of Physics and Center for Condensed Matter, Chinese Academy of Sciences, Beijing 100080, China*
(Received 26 September 1996)

The effects of field correlation on Raman-enhanced nondegenerate four-wave mixing (RENFWM) have been investigated by examining the RENFWM spectra as a function of time delay between two beams. We present a theory in which the underlying physics is emphasized. The field correlation has little influence on the RENFWM spectra when the laser has narrow bandwidth. In contrast, the ratio between the resonant and nonresonant RENFWM signal intensities increases as time delay is increased when the laser has broadband linewidth. Experiments with $CS_2$ as sample have been performed to demonstrate the field-correlation effects on the RENFWM spectra. [S1050-2947(97)07202-8]

PACS number(s): 42.65.Dr, 42.65.Hw

## I. INTRODUCTION

For years, a large amount of work has been devoted to the effects of laser field fluctuations on nonlinear optics. It now is well known that the influence of laser linewidths is more than just providing an additional broadening mechanism when the signal depends on higher than second order electric-field correlation [1]. Recently, much attention has been paid to the four-wave mixing (FWM) with correlated fields. Optical transients induced by time-delayed correlated fluctuating pulses have been proved to be a powerful technique in obtaining subpicosecond time resolution [2]. This time resolution is determined by the coherence time of the fluctuating field. The field correlation can also affect one-photon and two-photon transitions. In the case of a nearly Lorentzian laser power spectrum, the width of the two-photon absorption spectrum is decreased when the counter-propagating laser beams are partially decorrelated [3]. On the other hand, in an experiment of probe absorption due to atoms saturated by the strong pump, gain was observed when there was a time delay between the phase-diffusing pump and probe [4].

Coherent anti-Stokes Raman spectroscopy (CARS) is a nonlinear optical technique that is widely used for studying the vibrational or rotational mode of a molecule. The effects of laser field statistics on CARS have been studied by several research groups [5]. Recently, Rahn *et al.* [6] performed a crossed-beam, two-color CARS experiment to study the effects of field correlation on CARS spectra. They found that the ratio between the resonant and nonresonant CARS signal intensities changed as the time delay between pump beams was varied. These results demonstrate the non-Gaussian nature of the laser field statistics [6,7]. Although not as commonly used as CARS, Raman-enhanced nondegenerate four-wave mixing (RENFWM) possesses the advantages of nonresonant background suppression, excellent spatial resolution, free choice of interaction volume, and simple optical alignment [8]. Furthermore, there are three incident beams involved in RENFWM in which two of them originate from a single laser source. Therefore, by its very nature, RENFWM offers the possibility of studying the effect of field correlation. We have used a time-delayed method that employs the intrinsic incoherence of the pump beams and the order-of-magnitude difference between the relaxation time of the molecular-reorientational grating and the thermal grating to suppress the thermal background in the RENFWM spectrum [9,10]. We have also performed time-delayed RENFWM with incoherent light to measure the vibrational dephasing time [11]. In this paper, we study the effect of field correlation on RENFWM by measuring the time-delayed dependence of the RENFWM spectrum. The field correlation has little influence on the RENFWM spectra when the laser has narrow bandwidth. In contrast, the ratio between the resonant and nonresonant RENFWM signal intensities increases as time delay is increased when the laser has broadband linewidth. These can be explained by considering that the field fluctuations have different effects on the Raman resonance and on the laser-induced molecular-reorientational grating.

This paper is organized as follows. In Sec. II we present a theory of field-correlation effects on the RENFWM spectra. The underlying physics is emphasized here. In Sec. III the experimental setup and the results of RENFWM with correlated fields are presented. Section IV is the discussion and conclusion.

## II. THEORY

RENFWM is a third-order nonlinear phenomenon with three incident beams involved [8]. Beams 1 and 2 have the same frequency $\omega_1$ and a small angle exists between them. Beam 3 with frequency $\omega_3$ is almost propagating along the opposite direction of beam 1. In a Kerr medium, the nonlinear interaction of beams 1 and 2 with the medium gives rise to a molecular-reorientational grating. The FWM signal is the result of the diffraction of beam 3 by the grating. Now, if $|\omega_1-\omega_3|$ is near the Raman resonant frequency $\omega_R$, a moving grating formed by the interference of beams 2 and 3 will excite the Raman-active vibrational mode of the medium and enhance the FWM signal. The FWM signal (beam 4) has

*Author to whom correspondence should be addressed.

 

frequency $\omega_3$ and is propagating along the opposite direction of beam 2 approximately.

According to Ref. [10] the total polarization, which is responsible for the RENFWM signal, is given by

$$P(\mathbf{r},t)=P_M(\mathbf{r},t)+P_R(\mathbf{r},t), \tag{1}$$

with

$$P_M(\mathbf{r},t)=S(\mathbf{r},t)\chi_M\gamma_M A_3(t)\int_0^\infty dt'\ A_1(t-t') \times A_2^*(t-t')\exp(-\gamma_M t'), \tag{2}$$

$$P_R(\mathbf{r},t)=iS(\mathbf{r},t)\chi_R\gamma_R A_1(t)\int_0^\infty dt'\ A_2^*(t-t') \times A_3(t-t')\exp[-(\gamma_R-i\Delta)t']. \tag{3}$$

Here, $P_M(\mathbf{r},t)$ and $P_R(\mathbf{r},t)$ are the nonlinear polarizations originating from the molecular-reorientational grating and Raman-active mode, respectively; $\Delta=(\omega_1-\omega_3)-\omega_R$; $S(\mathbf{r},t)=\exp\{i[(\mathbf{k}_1-\mathbf{k}_2+\mathbf{k}_3)\cdot\mathbf{r}-\omega_3 t]\}$; $\mathbf{k}_i$ and $A_i(t)$ are the wave vector and the field magnitude of the $i$th beam, respectively; $\gamma_R$ and $\chi_R$ ($\gamma_M$ and $\chi_M$) are the relaxation rate and the nonlinear susceptibility of the Raman-active mode (molecular-reorientational grating), respectively. Physically, integration effects are involved in the establishment of both the molecular-reorientational grating and the Raman-active mode. The integrals in Eqs. (2) and (3) reflect these facts. On the other hand, the probing of the molecular-reorientational grating and the Raman-active mode are instantaneous processes. In our case, beams 1 and 2 come from a single laser source. Letting $\tau$ be the time delay of beam 2 with respect to beam 1, we have $A_1(t)=A(t)$, $A_2(t)=\xi A(t-\tau)$ with $\xi$ a constant. The RENFWM signal intensity, which is proportional to the average of the absolute square of the polarization over the random variable of the stochastic process, can be expressed as

$$I(\Delta,\tau)\propto\chi_M^2F_M(\tau)+\chi_R^2F_R(\Delta,\tau)-2\chi_M\chi_RF_{RM}(\Delta,\tau). \tag{4}$$

Here, $F_M(\tau)$, $F_R(\Delta,\tau)$, and $F_{RM}(\Delta,\tau)$ are functions which correspond to the FWM signal originating from the molecular-reorientational grating, the Raman-active mode, and the interference between the molecular-reorientational grating and the Raman resonance, respectively.

$F_M(\tau)$, $F_R(\Delta,\tau)$, and $F_{RM}(\Delta,\tau)$depend on the statistics of the laser fields. We assume that the lasers are multimode thermal sources with Lorentzian line shape, which satisfy Gaussian statistics. In this case $F_R(\Delta,\tau)$ and $F_{RM}(\Delta,\tau)$ are asymmetric about $\tau=0$. The expressions of $F_R(\Delta,\tau)$ and $F_{RM}(\Delta,\tau)$ are simple when beam 2 is temporally delayed from beam 1. In this case we have [10]

$$F_M(\tau)=\frac{\gamma_M}{\gamma_M+2\alpha}+\exp(-2\alpha|\tau|), \tag{5}$$

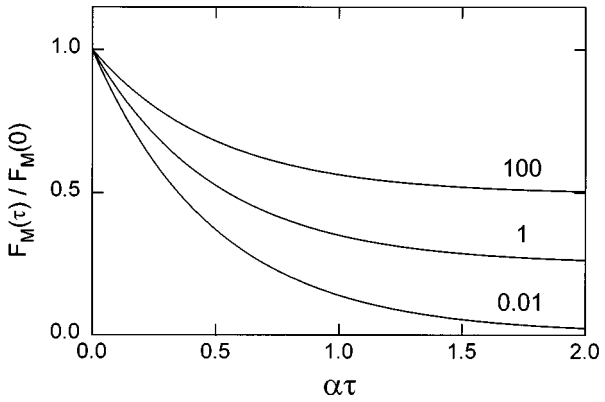


FIG. 1. Theoretical curves of $F_M(\tau)/F_M(0)$ vs $\alpha\tau$. Here the values of $\gamma_M/\alpha$, which equal 100, 1, and 0.01, are given.

$$F_R(\Delta,\tau)=\frac{\gamma_R(\gamma_R+\alpha+\alpha_3)}{(\gamma_R+\alpha+\alpha_3)^2+\Delta^2} \times\left[1+\exp(-2\alpha|\tau|)\left(\frac{\gamma_R}{\gamma_R+\alpha}\right)\right], \tag{6}$$

and

$$F_{RM}(\Delta,\tau)=\frac{\gamma_M\gamma_R\Delta}{(\gamma_M+\gamma_R+\alpha+\alpha_3)^2+\Delta^2} \times\left[\frac{\gamma_M+2(\gamma_R+\alpha+\alpha_3)}{(\gamma_R+\alpha+\alpha_3)^2+\Delta^2}+\frac{1}{\gamma_M+2\alpha}\right] +\exp(-2\alpha|\tau|)\left[\frac{\gamma_R\Delta}{(\gamma_R+\alpha+\alpha_3)^2+\Delta^2}\right]. \tag{7}$$

Here $\alpha=\delta\omega_1/2$ and $\alpha_3=\delta\omega_3/2$ with $\delta\omega_1$ and $\delta\omega_3$ the laser linewidth (full width at half maximum) of beams 1 and 3.

We first study the temporal behavior of the molecular-reorientational grating, which is induced by beams 1 and 2. Figure 1 presents theoretical curves of $F_M(\tau)/F_M(0)$versus $\alpha\tau$, where the values of $\gamma_M/\alpha$, which equal 100, 1, and 0.01, are given in the figure. The phase of the interference pattern of beams 1 and 2, i.e., the phase factor $\phi_M(\tau)$ of $A_1(t-t')A_2^*(t-t')$ in Eq. (2), changes from 0 to a random variable which fluctuates with a characteristic time scale of the laser coherence time $\tau_c\sim\alpha^{-1}$ when $\tau$ is varied from 0 to $\infty$. The effect of integration in the establishment of the molecular-reorientational grating, which last for a duration of approximately the relaxation time of the molecular-reorientational grating $\tau_M\sim\gamma_M^{-1}$, is to wash out the grating when $\tau\neq0$. When $\tau_M\gg\tau_c$ the molecular-reorientational grating will be washed out completely as $\tau\to\infty$ and we have $F_M(\tau)\propto\exp(-2\alpha|\tau|)$ in this limit (curve with $\gamma_M/\alpha=0.01$ in Fig. 1). In contrast, the integration effect does not affect the establishment of the grating when $\tau_M\ll\tau_c$. In this case, the molecular-reorientational grating becomes $\tau$ independent if the laser fields are only characterized by phase fluctuation [12]. For thermal sources with amplitude fluctuation, the coincidence of the intensity spikes between beams 1 and 2 gives rise to an enhancement of the amplitude of the molecular-reorientational grating at $\tau\simeq0$. More specifically,

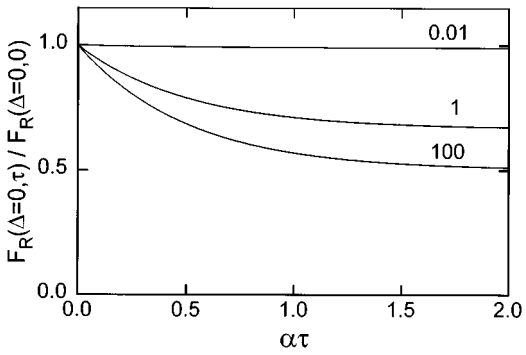


FIG. 2. Theoretical curves of $F_R(\Delta=0,\tau)/F_R(\Delta=0,0)$ vs $\alpha\tau$. Here the values of $\gamma_R/\alpha$, which equal 100, 1, and 0.01, are given.

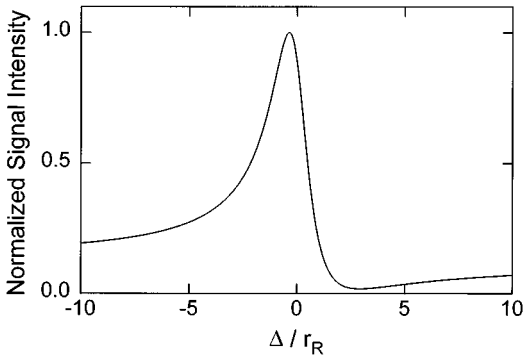


FIG. 3. Normalized RENFWM signal intensity vs $\Delta/\gamma_R$. Parameters: $\chi_M/\chi_R=0.4$, $\alpha/\gamma_R=\alpha_3/\gamma_R=0.01$, $\gamma_M/\gamma_R=2$, $\alpha\tau=0$. We note that for the narrow-band case the RENFWM spectrum does not depend on $\gamma_M/\gamma_R$ and $\alpha\tau$.

according to Eq. (5) we have $F_M(\tau)\propto 1+\exp(-2\alpha|\tau|)$when $\gamma_M \gg \alpha$ (curve with $\gamma_M/\alpha=100$ in Fig. 1).

We now consider the Raman resonant signal. Figure 2 presents theoretical curves of $F_R(\Delta=0,\tau)/F_R(\Delta=0,0)$ versus $\alpha\tau$, where the values of $\gamma_R/\alpha$, which equal 100, 1, and 0.01, are given in the figure. In contrast to the molecular-reorientational grating, the Raman-active mode is excited by the beat between beams 2 and 3. Although the phase factor $\phi_R$ of $A_2^*(t-t')A_3(t-t')$ in Eq. (3) is a stochastic variable, it is independent of $\tau$. Therefore, unlike the molecular-reorientational grating, the integration effect will not lead to the $\tau$ dependence of the normal coordinate $Q_R$ of the Raman-active mode, which is proportional to $\int_0^\infty dt'\, A_2^*(t-t')A_3(t-t')\exp[-(\gamma_R-i\Delta)t']$. Actually, $F_R(\Delta,\tau)$ is independent of $\tau$ if the laser sources are described by a phase-diffusion model [10]. For thermal sources the extra $\tau$-dependent part of $F_R(\Delta,\tau)$, which has the form $\exp(-2\alpha|\tau|)$, originates from the coincidence of the intensity spikes between $Q_R$ and the probe beam (beam 1). The magnitude of this $\tau$-dependent part can be estimated as follows. Consider the case where $\tau=0$. Due to the integration effect, $Q_R$ at time $t$ is the summation of the normal parameter induced at a time before $t$ for a duration of approximately $\tau_R\sim\gamma_R^{-1}$. However, only those parts of $Q_R$ induced during a time interval of approximately the laser coherence time $\tau_c$ of beam 2 can have intensity correlation with beam 1 and contribute to the $\tau$-dependent part of $F_R(\Delta,\tau)$. For $\tau_c \ll \tau_R$ (i.e., $\gamma_R \ll \alpha$), only $\tau_c/\tau_R$ of $Q_R$ is correlated with beam 1. Therefore, we have $F_R(\Delta,\tau)\propto 1+(\gamma_R/\alpha)\exp(-2\alpha|\tau|)$. Figure 2 shows that $F_R(\Delta=0,\tau)/F_R(\Delta=0,0)$ becomes almost independent of $\tau$ when $\gamma_R/\alpha=0.01$. Now we consider the case that $\tau_c \gg \tau_R$ (i.e., $\gamma_R \gg \alpha$). In this limit we have $Q_R$ fully correlated with beam 1, therefore, $F_R(\Delta,\tau)\propto 1+\exp(-2\alpha|\tau|)$ (curve with $\gamma_R/\alpha=100$ in Fig. 2).

We consider the RENFWM spectra when beams 1 and 2 have narrow bandwidth. Since both $F_M(\tau)$ and $F_R(\Delta,\tau)$ are proportional to $1+\exp(-2\alpha|\tau|)$ for $\gamma_M,\gamma_R \ll \alpha$, the ratio between them will not change as $\tau$ is varied. In order to fully understand the RENFWM spectrum it is also necessary to consider the relative phase between $P_M(t)$ and $P_R(t)$. The situation is simple when $\gamma_M,\gamma_R \gg \alpha$. In this case $A_1(t-t')A_2^*(t-t')$ and $A_2^*(t-t')$ in Eqs. (2) and (3) are slowly varying functions in comparison with $\exp(-\gamma_M t')$ and $\exp(-\gamma_R t')$, which have a peak at $t'=0$, and therefore can be approximated as $A_1(t)A_2^*(t)$ and $A_2^*(t)$, respectively. We have $P_M(t)$ and $P_R(t)$ proportional to $A_1(t)A_2^*(t)\int_0^\infty dt'\, A_3(t)\exp(-\gamma_M t')$ and $A_1(t)A_2^*(t)\int_0^\infty dt' A_3(t-t')\exp[-(\gamma_R-i\Delta)t']$, respectively. Although the phases of $P_M(t)$ and $P_R(t)$ fluctuate randomly, the relative phase between them does not depend on $\tau$. Combining with the feature of the constant ratio between the resonant and nonresonant signal, the RENFWM spectrum should not change as $\tau$ is varied. More specifically, in the limit of $\gamma_M,\gamma_R \gg \alpha$, we have

$$I(\Delta,\tau)\propto \chi_M^2+\chi_R^2\left[\frac{\gamma_R(\gamma_R+\alpha_3)}{(\gamma_R+\alpha_3)^2+\Delta^2}\right] -2\chi_R\chi_M\left[\frac{\gamma_R\Delta}{(\gamma_R+\alpha_3)^2+\Delta^2}\right]. \quad (8)$$

The above equation indicates that the RENFWM spectrum is independent of $\tau$ and the relaxation rate $\gamma_M$ plays no role here. In Fig. 3 we present the theoretical curve of the RENFWM spectrum when all incident beams are narrow-band lights ($\gamma_M,\gamma_R \gg \alpha,\alpha_3$). Parameters used are $\chi_M/\chi_R=0.4$, $\alpha/\gamma_R=\alpha_3/\gamma_R=0.01$. Although we set $\gamma_M/\gamma_R=2$ and $\alpha\tau=0$ in the calculation, the RENFWM spectrum is independent of the values of $\gamma_M/\gamma_R$ and $\alpha\tau$.

Now, we consider the case where beams 1 and 2 have broadband linewidth. For simplicity, we also assume that beam 3 is a narrow-band light. In other words, we consider the limit that $\alpha \gg \gamma_M$, $\gamma_R \gg \alpha_3$. At zero time delay no washout takes place in the establishment of the molecular-reorientational grating because $\phi_M(\tau=0)$ is stationary. On the other hand, due to the integration effect the fast random fluctuation of $\phi_R$ leads to the reduction of the amplitude of $Q_R$. As a result, comparing to the narrow-band case ($\gamma_M,\gamma_R \gg \alpha,\alpha_3$) the RENFWM spectrum exhibits a larger nonresonant background. Besides, the linewidth of the Raman resonant signal [full width at half maximum (FWHM)] increases from $2\gamma_R$ to $2\alpha$. We then increase $\tau$ so that beams 1 and 2 become uncorrelated. In this case, the randomization of $\phi_M(\tau)$ washes out the molecular-reorientational grating. In contrast, $F_F(\Delta,\tau)$ is nearly independent of $\tau$ because the $\tau$-dependent part of $F_R(\Delta,\tau)$ is much smaller than the $\tau$-independent part of $F_R(\Delta,\tau)$ when beams 1 and 2 have broadband linewidths. The implication of this is that the ratio

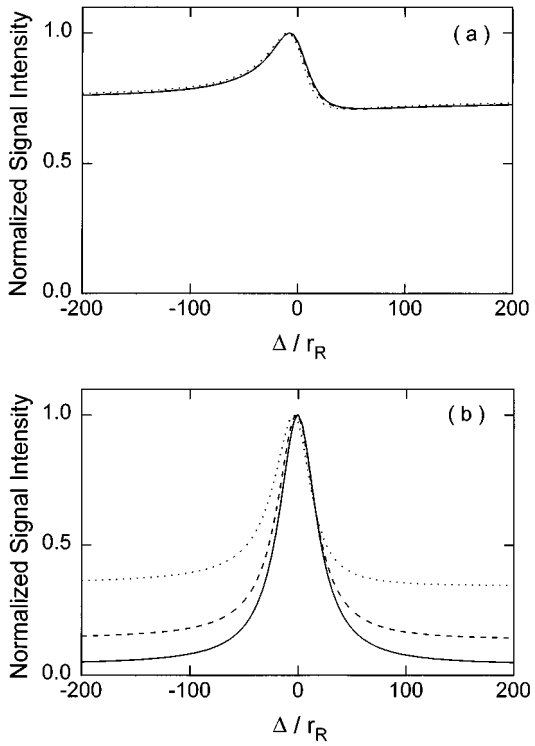


FIG. 4. Normalized RENFWM signal intensity vs $\Delta/\gamma_R$. Parameters: $\chi_M/\chi_R=0.4$, $\alpha/\gamma_R=20$, $\alpha_3/\gamma_R=0.01$, while $\alpha\tau=0$ for (a) and 10 for (b). Here $\gamma_M/\gamma_R=0.5$ (solid curve), 2 (dashed curve), and 8 (dotted curve).

between the nonresonant background and the Raman resonant signal decreases as $\tau$ is increased. To make this clear we define a parameter $\eta(\tau)=F_R(\Delta=0,\tau)/F_M(\tau)$, which reflects the $\tau$ dependence of the ratio between the resonant and nonresonant signal intensities. For the narrow-band case $(\gamma_M,\gamma_R\gg\alpha,\alpha_3)$, we have $\eta(\tau)=1$. When the laser linewidths of beams 1 and 2 change from narrow band to broadband $(\alpha\gg\gamma_M,\gamma_R\gg\alpha_3)$, $\eta$ at zero time delay is reduced by a factor of about $\gamma_R/\alpha$ [i.e., $\eta(0)\simeq\gamma_R/\alpha$], which is independent of $\gamma_M$. Now we increase the time delay between beams 1 and 2. In the limit of $\tau\rightarrow\infty$, we have $\eta(\tau\rightarrow\infty)\simeq 2\gamma_R/\gamma_M$. Since $\alpha\gg\gamma_M$ the nonresonant background is suppressed drastically and the RENFWM spectrum depends on the ratio between the relaxation rates $\gamma_R$ and $\gamma_M$. In Figs. 4(a) and 4(b) we present RENFWM spectra for $\alpha\tau=0$ and 10, respectively. Parameters used in these calculations are $\chi_M/\chi_R=0.4$, $\alpha/\gamma_R=20$, $\alpha_3/\gamma_R=0.01$; while $\gamma_M/\gamma_R=0.5$ (solid curve), 2 (dashed curve), and 8 (dotted curve). These parameters are the same as that used in Fig. 3 except $\alpha/\gamma_R$ is changed from 0.01 to 20. We note that for the narrow-band case the RENFWM spectrum does not depend on $\gamma_M/\gamma_R$. Comparing to the narrow-band case (Fig. 3), Fig. 4(a) shows a much larger nonresonant background. The nonresonant background is reduced as the time delay increases [Fig. 4(b)]. Furthermore, the nonresonant background decreases as $\gamma_M/\gamma_R$ decreases. Another interesting thing is that, when $\gamma_M/\gamma_R=2$ [dashed curve in Fig. 4(b)], we have $\eta(\tau\rightarrow\infty)=1$ for the broadband case, which is the same as that for the narrow-band case. However, the relative phase between $P_M(t)$ and $P_R(t)$ is now a stochastic variable. Due to the randomization of the relative phase between the Raman resonant term and the nonresonant background the interference between them disappears almost completely. As a result, RENFWM spectrum exhibits a symmetric line shape. As $\gamma_M/\gamma_R$ is decreased further so that $\gamma_M/\gamma_R<2$, the ratio between the resonant and nonresonant signal can even be enhanced in comparison with the narrow-band case [see solid curve in Fig. 4(b)]. Finally, we emphasize that since $\gamma_M/\alpha$ affects the washout of the molecular-reorientational grating, therefore, as demonstrated in Fig. 4(a), this parameter has little influence on the RENFWM spectrum at zero-time delay when the grating is stationary.

## III. EXPERIMENT

Previously, we have measured the vibrational relaxation time of $CS_2$ by time-delayed RENFWM with a broadband laser source [11]. Here, we study the effects of field correlation on the RENFWM spectrum again in $CS_2$. The difference between these two experiments is that for the former case, we study the temporal behavior of the FWM signal intensity with fixed frequency detuning. While for the latter case, we are interested in the RENFWM spectrum with fixed time delay. The relaxation rate of the 656-$cm^{-1}$ vibrational mode of $CS_2$ is $\gamma_R=5\times10^{10}$ $sec^{-1}$. On the other hand, as is well known, the optical Kerr effect for the liquid $CS_2$ has at least two components, i.e., a relatively long ''Debye'' component and a shorter ''interaction-induced'' component, which have relaxation times of about 2 ps and 300 fs, corresponding to relaxation rates of $5.0\times10^{11}$ and $3.3\times10^{12}$ $sec^{-1}$, respectively. To study the field-correlation effects for the broadband case, it is required that $\alpha\gg3.3\times10^{12}$ $sec^{-1}$. However, from a practical experimental consideration, here we chose $\alpha=1.8\times10^{11}$ $sec^{-1}$. This value is larger than $\gamma_R$ while smaller than the relaxation rate of the slow component of the molecular-reorientational grating. We found that the RENFWM spectrum showed a clear evidence of the field-correlation effect even when we were not in the broadband limit.

The experimental setup is similar to that described in Ref. [11]. We studied the 655.7-$cm^{-1}$ vibrational mode of carbon disulfide ($CS_2$) which was contained in a sample cell with thickness 10 mm. The second harmonic of a Quanta-Ray YAG laser was used to pump two dye lasers ($DL1$ and $DL2$). The linewidth of the first dye laser $DL1$ could be either 0.007 or 0.07 nm. This laser had wavelength 585 nm, output energy 1.5 mJ, and pulse width 5 ns. To obtain a light source with 0.07-nm linewidth, we used a simple cavity that consisted of a 1200-line/mm grating and an output mirror only with no optical component to expand the beam diameter. The laser output was split into beams 1 and 2 after passing through a beam splitter, and the two beams intersect in the sample with a small angle (1.3°) between them. Beam 3, originating from a narrow-band dye laser $DL2$ with linewidth 0.007 nm and output energy 1 mJ, propagated along the direction opposite to that of beam 1 The wavelength of beam 3 was approximately 563 nm and could be scanned by a computer-controlled stepping motor. All the incident beams were linearly polarized in the same direction. The FWM signal, which had the same polarization as the incident beams, propagated along a direction almost opposite to that of beam 2. In this experiment, all the incident beams were

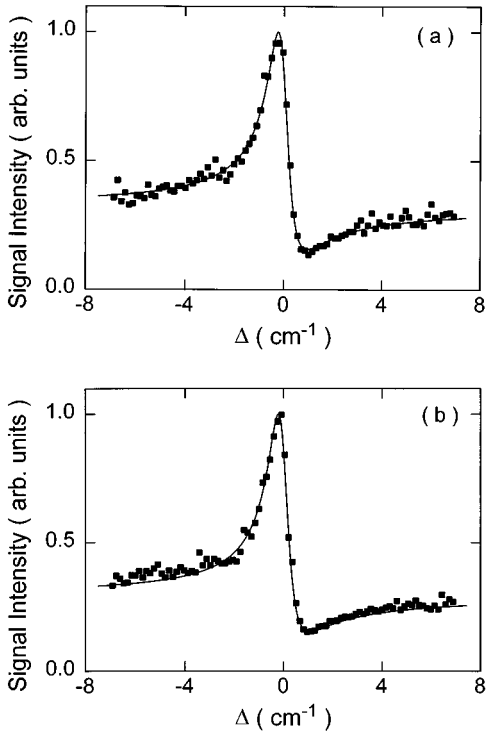


FIG. 5. The RENFWM spectra at $\tau=0$ ps for (a) and 5600 ps for (b) when $DL1$ has linewidth 0.007 nm. Solid curve: theoretical curve with $\gamma_R=5\times10^{10}$ sec$^{-1}$, $\gamma_{M1}=5\times10^{11}$ sec$^{-1}$, $\gamma_{M2}=3\times10^{12}$ sec$^{-1}$, $\chi_{M1}/\chi_R=0.35$, $\chi_{M2}/\chi_R=0.20$, $\alpha=\alpha_3=2\times10^{10}$ sec$^{-1}$; while $\tau=0$ ps for (a) and 5600 ps for (b).

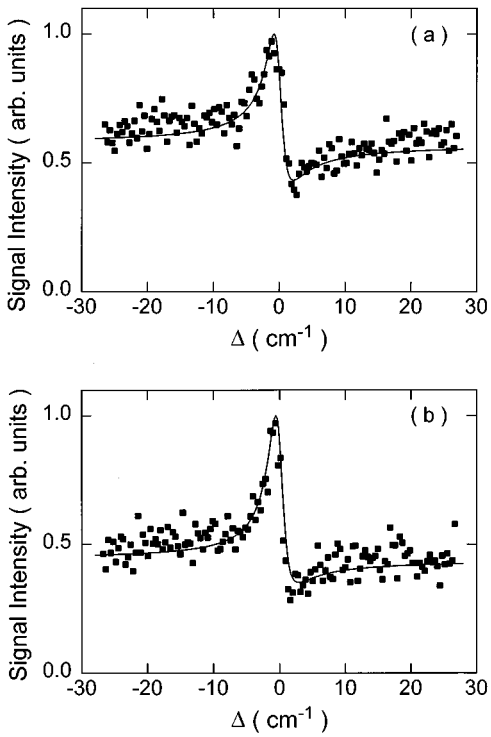


FIG. 6. The RENFWM spectra at $\tau=0$ ps for (a) and 1300 ps for (b) when $DL1$ has linewidth 0.07 nm. Solid curve: theoretical curve with $\gamma_R=5\times10^{10}$ sec$^{-1}$, $\gamma_{M1}=5\times10^{11}$ sec$^{-1}$, $\gamma_{M2}=3\times10^{12}$ sec$^{-1}$, $\chi_{M1}/\chi_R=0.35$, $\chi_{M2}/\chi_R=0.20$, $\alpha=1.8\times10^{11}$ sec$^{-1}$; $\alpha_3=2\times10^{10}$ sec$^{-1}$; while $\tau=0$ ps for (a) and 1300 ps for (b).

focused to spots with diameters of approximately 0.5 mm. The
RENFWM signal was detected by a photodiode and then fed into a signal averager for data averaging. A computer was used for data processing and for controlling the stepping motor to vary the wavelength of beam 3.

We first consider the case that $DL1$ is a narrow-band laser with linewidth 0.007 nm, which corresponds to a coherence time of about 50 ps. Figures 5(a) and 5(b) present the RENFWM spectra when $\tau=0$ and 5600 ps, respectively. Beams 1 and 2 are fully correlated when $\tau=0$ ps, whereas no correlation exists between beams 1 and 2 when $\tau=5600$ ps. It is found from Fig. 5 that the field correlation has little effect on the RENFWM spectrum when $DL1$ has narrow bandwidth. The situations become quite different when the linewidths of beams 1 and 2 are increased to 0.07 nm. Figures 6(a) and 6(b) present the RENFWM spectra when $\tau=0$ and 1300 ps, respectively. Comparing to the full correlation case [Fig. 6(a)], the nonresonant background decreases and the intensity profile changes as beams 1 and 2 become uncorrelated [Fig. 6(b)].

As mentioned before, the optical Kerr effect of $CS_2$ has a long ''Debye'' and short ''interaction-induced'' components. In Ref. [10] we have established a RENFWM theory, where the nonresonant background originated from molecular-reorientational grating and thermal grating. This theory is ready to explain the experimental results in $CS_2$. We used Eq. (8) in Ref. [10] to fit our data with $\gamma_M$ and $\gamma_T$ ($\chi_M$ and $\chi_T$) in Eq. (8) replaced by $\gamma_{M1}$ and $\gamma_{M2}$ ($\chi_{M1}$ and $\chi_{M2}$), respectively. Here, $\gamma_{M1}$ and $\gamma_{M2}$ ($\chi_{M1}$ and $\chi_{M2}$) are the relaxation rates (nonlinear susceptibilities) of the Debye and interaction-induced components, respectively. The solid curves in Figs. 5 and 6 are the theoretical curves. Parameters used are $\gamma_R=5\times10^{10}$ sec$^{-1}$, $\gamma_{M1}=5\times10^{11}$ sec$^{-1}$, $\gamma_{M2}=3\times10^{12}$ sec$^{-1}$, $\chi_{M1}/\chi_R=0.35$, $\chi_{M2}/\chi_R=0.20$, $\alpha_3=2\times10^{10}$ sec$^{-1}$; while $\alpha=2\times10^{10}$ sec$^{-1}$ for Fig. 5 and $1.8\times10^{11}$ sec$^{-1}$ for Fig. 6. The time delays are $\tau=0$ and 5600 ps ($\tau=0$ and 1300 ps) for Figs. 5(a) and 5(b) [Figs. 6(a) and 6(b)], respectively. The agreement between the experimental data and theoretical curves is satisfactory.

Finally, we note that the laser linewidth can be increased to about 4.0 nm if we use a simple laser cavity, which consisted of a total reflection end mirror and an output mirror with 8% reflection. We have $\alpha=1\times10^{13}$ sec$^{-1}$, which is larger than the relaxation rate of the fast component of the optical Kerr effect. To obtain a whole RENFWM spectrum, it is required that the frequency detuning is scanned for a range of about $20\alpha$ (see Fig. 4), or 40 nm in this case. The problem here is that, due to the frequency dependence of the laser output, it is difficult to obtain reliable data with such a large frequency scanning.

## IV. DISCUSSION AND CONCLUSION

In the crossed-beam, two-color CARS experiments Rahn *et al.* [6] found a similar reduction of the nonresonant background as the time delay increased when the laser linewidth was much larger than the relaxation rate of the Raman mode. Although crossed-beam, two-color CARS and RENFWM are both FWM with signal enhanced by the Raman resonance, the basic physics underlying are quite different. More spe-

cifically, the signal frequency of CARS is $\omega_1+\omega_1-\omega_3$, which means that a photon is absorbed from each of the two mutually correlated pump beams. On the other hand, the signal frequency of RENFWM is $\omega_1-\omega_1+\omega_3$, therefore photons are absorbed from and emitted to the mutually correlated beams 1 and 2, respectively. This difference has a profound influence on the field-correlation effects. For example, in the time-delayed coherent Stokes Raman scattering (CSRS) with incoherent light, where CSRS has the same physical principle as CARS, the delay-time dependence of the CSRS signal is symmetric and exhibits a coherent spike at zero time delay [13]. In contrast, no coherent spike appears at $\tau=0$ in the corresponding time-delayed RENFWM with incoherent light and the temporal behavior of RENFWM is asymmetric [11]. Now, we consider the time-delayed dependence of the CARS spectrum. We assume that the pump beams, which have Lorentzian line shapes, satisfy Gaussian statistics. It can be shown that, although the Raman term and the nonresonant background have different $\tau$ dependence, the signal intensities at $\tau=0$ for both of them have an enhancement of a factor of 2 compared to that at $\tau=\infty$. Therefore, for Gaussian theory the ratios between the resonant and nonresonant CARS signal intensities are the same for $\tau=0$ and $\tau\rightarrow\infty$. This behavior is completely different from that in RENFWM. The reduction of the nonresonant background at large time delay in the crossed-beam, two-color CARS experiment is attributed to the non-Gaussian nature of the laser field statistics [6,7].

In conclusion, the effects of field correlation on RENFWM have been investigated by examining the $\tau$ dependence of the RENFWM spectra. We present a theory in which the underlying physics is emphasized. The field correlation has little influence on the RENFWM spectra for the narrow-band case. In contrast, for the broadband case the ratio between the resonant and nonresonant RENFWM signal intensities increases as $\tau$ is increased. Experiments with $CS_2$ as sample have been performed to demonstrate the field-correlation effects on the RENFWM spectra.

## ACKNOWLEDGMENTS

The authors gratefully acknowledge the financial support from the Chinese National Nature Sciences Foundation and the climbing program from the Chinese Commission of Science and Technology.

[1] D. S. Elliott, M. W. Hamilton, K. E. Arnett, and S. J. Smith, Phys. Rev. Lett. **53**, 439 (1984); Ce Chen, D. S. Elliott, and M. W. Hamilton, *ibid.* **68**, 3531 (1992).

[2] R. Beach and S. R. Hartmann, Phys. Rev. Lett. **53**, 663 (1984); N. Morita and T. Yajima, Phys. Rev. A **30**, 2525 (1984); S. Asaka, H. Nakatsuka, M. Fujiwara, and M. Matsuoka, *ibid*. **29**, 2286 (1984); G. S. Agarwal, *ibid*. **37**, 4741 (1988).

[3] D. S. Elliott, M. W. Hamilton, K. Arnett, and S. J. Smith, Phys. Rev. A **32**, 887 (1985).

[4] M. H. Anderson, G. Vemuri, J. Cooper, P. Zoller, and S. J. Smith, Phys. Rev. A **47**, 3202 (1993).

[5] M. A. Yuratich, Mol. Phys. **38**, 625 (1979); G. S. Agarwal and S. Singh, Phys. Rev. A **25**, 3195 (1982).

[6] L. A. Rahn, R. L. Farrow, and R. P. Lucht, Opt. Lett. **9**, 223 (1984).

[7] G. S. Agarwal and R. L. Farrow, J. Opt. Soc. Am. B **3**, 1596 (1986).

[8] Z. Yu, X. Lu, P. Ye, and P. Fu, Opt. Commun. **61**, 287 (1987).

[9] Z. Yu, X. Mi, Q. Jiang, P. Ye, and P. Fu, Opt. Lett. **13**, 117 (1988); Z. Yu, X. Mi, Q. Jiang, and P. Fu, Opt. Commun. **107**, 120 (1994).

[10] P. Fu, Z. Yu, X. Mi, Q. Jiang, and Z. Zhang, Phys. Rev. A **46**, 1530 (1992).

[11] X. Mi, Z. Yu, Q. Jiang, and P. Fu, Phys. Rev. A **48**, 3203 (1993).

[12] P. Fu, Z. Yu, X. Mi, and P. Ye, J. Phys. (Paris) **48**, 2089 (1987).

[13] T. Hattori, A. Terasaki, and T. Kobayashi, Phys. Rev. A **35**, 715 (1987).